Principles of lipid – enzyme interactions in the limbus region of the catalytic site of Candida antarctica Lipase B

# Principles of lipid – enzyme interactions in the limbus region of the catalytic site of *Candida antarctica* Lipase B

Lucia Silvestrini[a] and Michele Cianci[a]

[a]Department of Agricultural, Food and Environmental Sciences, Università Politecnica delle Marche, Via Brecce Bianche, 60131 Ancona (Italy)

*Corresponding e-mail: m.cianci@univpm.it

**ABSTRACT:** Lipases (E.C. 3.1.1.3) are ubiquitous hydrolases for the carboxyl ester bond of water-insoluble substrates such as triacylglycerols and phospholipids. *Candida antarctica* Lipase B (CALB) acts in aqueous as well as in low-water media, thus being of considerable biochemical significance with high interest also for its industrial applications.

The hydrolysis reaction follows a two-step mechanism, or 'interfacial activation', with adsorption of the enzyme to a heterogeneous interface and subsequent enhancement of the lipolytic activity. Once positioned within the catalytic triad, substrates are then hydrolysed, and products released. However, the intermediate steps of substrate transfer from the lipidic-aqueous phase to the enzyme surface and then down to the catalytic site are still unclear.

By inhibiting CALB with ethyl phosphonate and incubating with glyceryl tributyrate (2,3-di(butanoyloxy)propyl butanoate), the crystal structure of the lipid-enzyme complex, at 1.55 Å resolution, shows the tributyrin in the limbus region of active site. The substrate is found 10 Å above the catalytic Ser, with the glycerol backbone pre-aligned for further processing by key interactions via an extended water network with α-helix10 and α-helix5.

The findings offer new elements to elucidate the mechanism of substrate recognition, transfer and catalysis of *Candida antarctica* Lipase B (CALB) and lipases in general.

**KEYWORDS:** Lipase; fatty acid metabolism; lipid chemistry; interfacial enzymology; tributyrin; CALB.

## 1. INTRODUCTION

Many enzymes, both in the living world and in biotechnological processes, work at interfaces such as cell membranes, surfaces like endothelium or beads in a reactor, or oil-water interfaces. With a soluble enzyme acting on an insoluble substrate, the partitioning of the substrate between the aqueous and non-aqueous phase is a key factor. Little is known about the intermediate steps of substrate transfer from the interface down to the core of an enzyme. In fact, chemical understanding of prior substrate recognition and positioning at enzyme surface are still lacking, while being of considerable interest to unveil enzyme functioning.

Lipases (E.C. 3.1.1.3) are ubiquitous enzymes of considerable physiological significance with high interest for their industrial applications being capable of catalysing many different reactions, such as hydrolysis or synthesis of esters, esterifications, aminations, transesterifications, alcoholysis, among others [1, 2]. Due to lipase versatility front of many substrates, the application of these enzymes extends to various sectors, such as synthesis reactions, production of pharmaceutical drugs and biofuels, among others [2-5]. The hydrolysis reaction, in aqueous as well as in low-water media, for the carboxyl ester bond of water-insoluble substrates as triacylglycerols, oil, fats, and other insoluble substrates, follows adsorption of the enzyme to an heterogeneous interface and subsequent enhancement of the lipolytic activity, defined as 'interfacial activation' [6-9]. Specificity and selectivity of lipases are readily modulated by genetic manipulation or physio-chemical modifications, like immobilization [5, 10-14], therefore studying and understanding of lipase enzymatic mechanism requires several perspectives.

Among lipases, *Candida antarctica* Lipase B (CALB) is widely applied to many industrial processes for its high enantioselectivity, range of substrates, thermal stability, and stability in organic solvents [15, 16]. CALB belongs to the α/β hydrolase fold family with a conserved catalytic Ser-Asp-His triad [17-19]. The protonation state of the catalytic triad has also been established [17, 20].

Studies on the interfacial activity of CALB have so far focused on the lid regions. CALB has two

α-helices surrounding the active site, namely α5 and α10 [17, 18] which have been shown to be very flexible and could work as a lipase lid by a relative motion between them either by increasing the working temperature [21] or by working in organic solvents [22]. The CALB sequence stretch around the α-helix 5 has been shown to significantly influence the catalytic properties of the enzyme, including the enantioselectivity, which, consequently, seems to be not exclusively directed by the fit of the substrate into the enzyme's active site pocket [23].

Substrate – protein interactions in *Candida antarctica* Lipase B, and in lipases in general are therefore of great interest for the understanding of the reaction mechanism of these enzymes. There are working models for how CALB interacts with triglyceride-water interfaces [24, 25]. The positioning of the substrate in proximity of the Ser105 and the consequences for substrate selectivity and stereospecificity have been revealed and discussed by Uppenberg et al. [18]. Hydrolysis of tributyrin can be considered a model reaction since it can be performed either in water-tributyrin emulsion with free lipase as catalyst or in neat tributyrin with absorbed lipase [26]. In fact, absorbed CALB showed 49% of the activity shown in the emulsion system, proving that it can work well in both conditions [27]. There is, however, no structural information about the intermediate steps of substrate transfer from the lipid/water phase firstly to the enzyme surface and then down to the active site. Structural description of the lipid positioning at the protein surface is then of considerable interest for the understanding of several aspects of lipase functioning and enzymes in general.

The first results in this direction have been the crystal structure of CALB-phosphonate inhibitor complex (PDB code: 1LBS) obtained by Uppenberg et al. [18]. The complex, presented here, goes beyond that structure by describing at the atomic level hydrophobic and hydrophilic interactions of a tributyrate molecule with the opening or limbus region of the active site of a commercial preparation of CALB from Hampton Research.

## 2. MATERIALS AND METHODS

### 2.1. Enzyme preparation and inhibition

*Candida antarctica* Lipase B (CALB), purchased from Hampton Research (catalogue number HR7-009), was the product of submerged fermentation of a genetically modified *Aspergillus oryzae* microorganism, and delivered as a white crystal powder with no other ingredients or buffering salts. No further purification steps were performed prior to crystallization trials. A 15 mg/mL CALB solution in 20mM Na($CH_3COO$) pH = 4.8 was incubated with a solution of paraoxon-ethyl (SIGMA catalog n. N12816) 30mM in water for one day at room temperature. Since paraoxon-ethyl is a phosphonate inhibitor, a well know class of tested lipase inhibitors [18, 28] no enzymatic activity assay was deemed as necessary.

### 2.2. Enzyme crystallization

Crystallization trials were performed at 293 K using the hanging-drop method using a Qiagen™ EasyXtal 15-well plate. 1 µL of CALB solution was diluted with 1 µL of the precipitant solution, made of 200mM Na($CH_3COO$) pH = 4.8, 20% (w/v) PEG4000 (SIGMA catalogue n. 81240), and 15% (v/v) glyceryl tributyrate (SIGMA catalogue n. T8626). The drop was equilibrated by vapor diffusion against 500 µL of the precipitant solution and the crystallization plate was stored at 293 K. Protein crystals of the glycerol tributyrate-CALB complex appeared within two weeks and grew to a size of $0.1 \times 0.1 \times 0.05$ $mm^3$ in five weeks.

### 2.3. X-ray diffraction data collection and structure analysis

Diffraction data were collected at 100 K using synchrotron radiation at the EMBL P13 beamline at the Petra III storage ring, c/o DESY, Hamburg (Germany) [29]. Crystals were cooled at 100 K with a cold nitrogen stream. The wavelength was set to 0.826 Å, using a Si(III) crystal monochromator

(FMB-Oxford). The data were integrated using the program XDS [30] and scaled with AIMLESS [31]. Crystal diffracted to 1.55 Å resolution with unit cell dimensions of a = 86.4 Å, b = 156.6 Å, and c = 138.8 Å and space group $C222_1$. Data collection statistics are reported in Table 1.

The structure of glycerol tributyrate-CALB complex was solved by molecular replacement using MOLREP [32] starting from the deposited structure of CALB as search model (Protein Data Bank (PDB): 1TCA [17]). The models were subjected to rigid-body minimization and subsequently to refinement steps with REFMAC [33] with isotropic temperature factors refinement and automatic weighting scheme. Manual rebuilding of the models were performed using the COOT graphic interface [34] by inspecting the electron density map, calculated with $2F_{obs}$-$F_{calc}$ or $F_{obs}$-$F_{calc}$ coefficients and phases calculated from the model. Models were validated using the PDB_REDO web server [35] and finally refined using the PHENIX crystallographic suite [36], with occupancy refinement of the ligands. The structure was refined to a $R_{factor}$ and $R_{free}$ (5% of data) of 16.3% and 19.2 %. Refinement statistics are reported in Table 2.

## 3. RESULTS

Equilibrating CALB, inhibited by paraoxon-ethyl, against a solution containing 15% (v/v) glyceryl tributyrate yielded crystals suitable for X-ray analysis. The refined crystallographic model, at 1.55 Å resolution shows the typical tertiary structure of CALB, closely matching the open conformation of native CALB (chain A, PDB code 5A71, [20]) with a backbone RMSD of 0.35 Å.

There are three CALB monomers (chain A, B and C) in the asymmetric unit, of which chain A and B form a dimer within the asymmetric unit and the third one, chain C, forms a dimer with the C' chain from a symmetry related unit. The diethyl-phosphonate moiety (DEP) bound to Ser105, produced by paraoxon-ethyl inhibition, shown by the unbiased omit electron density map, occludes access to the catalytic triad.

In both dimers the presence of a glyceryl tributyrate molecule at a bridge position between two monomers (Figure 1a) is identified via the unbiased omit electron density map (Figure 1b and 1c). The refined occupancy for the two glyceryl tributyrate molecules is 1.00 corresponding at a fully loaded enzyme. The glyceryl tributyrate molecule is suspended above the active site where the Ser105 forms the acyl complex with diethyl-phosphonate moiety and it interacts with the β-turn region between the β-strands β6 and β7 via an extended water network and with α-helix10 and α-helix5 with several hydrophobic interactions. The side chains of Leu278, Ala282, Ile285 and Val286 of α-helix 10 are within Van der Waals distance from the 1- and 2- fatty acid aliphatic chains of the glyceryl tributyrate. The side chains of Leu140, Ala141, Leu144 of α-helix5 and Val154 of α-helix6 are arranged towards the substrate and maintain the hydrophobic character for the upper surrounding of the cavity (Figure 1d).

The carbonyl groups of the peptide bonds of Glu188, Ile189, Leu140 and Val149 tether several water molecules which, in turn, form hydrogen bonds with the moiety groups of glyceryl tributyrate. The arrangement of the water molecules, polar and hydrophobic residues on the CALB surface (Figure 1d and 1e) is clearly reflected in an electrostatic potential defining three regions

corresponding to α-helix5 (polar and apolar), α-helix10 (hydrophobic) and the β-turn region between the β-strands β6 and β7 (polar) on which triglyceride sits with the glycerol backbone towards the α-helix5 and the β-turn and with the aliphatic chain towards α-helix10 (hydrophobic) (Figure 1f).

In this crystal structure the fatty acid aliphatic chain bound to the glyceryl tributyrate in position 3- generates interactions with the second monomer of the homodimer (Figure 1d), thus creating the conditions for the formation of the homodimer observed in the crystallographic structure. The buried surface area and the free dissociation energy for the homodimer including glycerol tributyrate, calculated using PISA [37], are 1065 $Å^2$ and 21.2 kcal mol-1 with the main regions of buried surface area being α-helix5, α-helix10 and the β-turn region between the β-strands β6 and β7.

The interactions of the glyceryl tributyrate molecule with the two CALB molecules are basically equivalent with the overall positioning of the glyceryl tributyrate molecule within the upper level of the active site, interacting with the aliphatic region of α-helix10. The same nature of substrate-protein interactions is observed within monomer C and the opposite, symmetry related, protein molecule.

## 4. DISCUSSION

In this study we investigated the nature of the very first level of lipid interaction with a lipase defining an intermediate region between the environment and the active site, where the first recognition of the substrate occurs. An inhibited enzyme was used to exclude the presence of deposits of reaction products accumulated anywhere. The substrate was free to diffuse in solution as proved by the fact that we could observe only electron density on the protein surface which could

be unambiguously assigned to tributyrin. On the other hand no other electron densities were observed which could be assigned to accumulated reaction products.

Variations of temperature and pH can affect the hydrophobic and hydrophilic interactions of an enzyme due to stabilization or destabilization of secondary or tertiary structure [38]. The optimal pH for catalysis of CALB is 7, and the enzyme is stable in aqueous media in the range of pH 3.5-9.5 [15] with a theoretical isoelectric point (pI) of 5.8. The crystallization conditions used here are very similar to the reported conditions by Uppenberg et al. [39] and very close to the ones reported by Stauch et al. [20] which resulted in a fully conserved enzyme structure showing the lid in both open and closed form. In particular, the pH used for crystallization is 4.8, and a value that is just above the pKa of the side chain of Asp187 (pKa = 3.86) residue. In these conditions it was observed that, for both the open and the closed forms, Asp187 was deprotonated and His224 was single protonated [20]. These protonation states are necessary for enzymatic activity, and would be preserved at pH higher than the pI. The reasons for the activity change can then be sought for elsewhere. It was already noted that, raising the pH from 3.6 to 5.5 would cause α-helix 10 change from an ordered structure to disordered structure, manifested by a lack of continuous electron density [17]. Chimeras of *Candida antarctica* lipase B displayed large variations in kinetic constants and enantiomeric ratio for hydrolysis of p-nitrophenyl esters by lid swapping [23]. It is noteworthy that the removal of the Asp145 from α-helix 5 region in the chimeras of *Candida antarctica* lipase B, removed the activity pH dependence [23], clearly indicating a relationship between optimal activity pH and primary sequence of the lid region.

The position of α-helix5 and α-helix10 is modulated by the dielectric properties of the surrounding media and it varies the surface area and the hydropathicity of the upper level of the catalytic cavity as discussed by several authors [20, 24, 25, 40]. Further to the report that CALB indeed has a lid [20] and that it shows an ‘interfacial activation’ mechanism on highly hydrophobic surfaces with bulky substrates [24], it has also been proposed that activation occurs when the binding free energy

between the lid and a hydrophobic surface is larger than a critical value of 4.0 kcal $mol^{-1}$, which is the one between the lid and the lid-holder [41]. The fact that the open conformation of CALB we observe in presence of tributyrate and of the phosphonate inhibitor, presented here, is highly similar with the open conformation of CALB observed in absence of tributyrate and phosphonate [20], supports the thesis that the surface area and the hydropathicity of the upper level of the catalytic cavity, that is physically generated by the position of α-helix5 and α-helix10, is modulated by the dielectric properties of the surrounding media [20, 24, 25, 40]. The lid region itself, with its primary (amino acid composition and number of residues) and secondary structure can modulate the 'interfacial activation behaviour' of CALB [20, 24].

The thermal stability, the mobility of the enzyme lid, water accessibility and mass transfer are then key parameters for the enzyme preparation strategy [4, 13, 42, 43], especially in the design and application of support matrixes for lipases [12, 44] [45] to enhance enzyme activity and reusability. While for the crystallization conditions reported by Stauch et al., [20] 10-13 % (v/v) 2-propanol was part of the precipitant solution, here 15% (v/v) glyceryl tributyrate was used instead. Given the limited solubility of glyceryl tributyrate in water of 0.13 mg/mL at 312 K, upon mixing the protein solution and the precipitant solution in ration 1:1 for a final volume of 2 µL, an emulsion was obtained with several microdroplets of fat, visible at the microscope. After resting for the five weeks at 293 K, crystals grew within the emulsion. The observed presence of glyceryl tributyrate molecule on the enzyme surface (Figure 1), confirms that the emulsion formation in the crystallization droplets was not a limiting factor for the diffusion of the substrate to reach the enzyme surface. Moreover, the fact that the refined occupancy for the glyceryl tributyrate molecules was 1.00 corresponding at a fully loaded enzyme, indicates that crystallization conditions were adequate to overcome any possible diffusion limitation within the crystallization droplets.

The structure reported here sheds light into why CALB shows a total stereoselectivity for sn-1,3 when using tributyrin as substrate [46]. By inspecting all the possible orientations of tributyrin over the active site observed in the crystal structure, as generated by symmetry (Figure 1e), we can observe that, firstly, the position of the glycerol backbone is conserved, and in particular the positioning of sn-2 is invariant with respect to all the possible orientation of the tributyrin molecule. Secondly, the aliphatic chain of the fatty acid in position sn-2 (Figure 1d, 1e and 1f), is uniquely oriented towards the Ala279 of α-helix10, while the aliphatic chains of the fatty acids in position sn-1 and sn-3 present a certain degree of freedom. The fatty acid in position sn-1 is seemingly floating in the wide acyl side of the cavity, and the aliphatic chain of the fatty acid in position sn-3 floats in the open media (Figure 1e,f). Notably, the position of the butanolyoxy group in sn-2 appears to have a pivotal role when the triglyceride is approaching to the serine of the CALB, when a transition state takes place and the first acyl enzyme and a diglyceride are formed. Finally, no significantly different orientations of the amino acid side chains within the cavities could be noted from the open conformation CALB structure reported by [20].

The recognition of the lipid within the lipase is determined by three main contributions. The first contribution is the hydrophilic one, generated by the carbonyl groups of the peptide bonds of the β-turn region between the β-strands β6 and β7 tethering water molecules which, in turn, form hydrogen bonds with the moiety groups of glyceryl tributyrate holding the glycerol backbone. The second contribution is the hydrophobic one generated by the side chains of α-helix10 and from α-helix5 generating a hydrophobic "bed" for the 1- and 2- fatty acid aliphatic chains of the glyceryl tributyrate. The region defined by Leu144, Val154, Ile189, Leu219, Val221, Ala281, Ala282, Ile285, Leu287 was already shown able to bind Xenon atoms [20], thus confirming the hydrophobic nature of the cavity. It has been discussed by Zisis et al., [24] that a highly open conformation is favoured in a hydrophobic environment and this conformation is required for binding large, bulky substrates. Moreover, the interfacial activation of CALB is evident on highly hydrophobic surfaces

with large, bulky substrates. In this case, CALB, an esterase for small substrates, acts like as a lipase with large conformational change of α-helix5 [24]. Several crystal structures of CALB have shown α-helix5 adopting open and closed [20] and intermediate [18] conformations, showing the flexibility of this region. The side chains of α-helix5, matching the open conformation, are beyond Van der Waals distance from the substrate (Figure 1f), so not directly interacting with it. This evidence explains why CALB behaves as an esterase for small substrates like glyceryl tributyrate and as a lipase for larger substrates.

The third contribution is coming from the presence of water molecules tethered by the carbonyl groups of the peptide bonds of Glu188, Ile189, Leu140 and Val149, thus forming hydrogen bonds with the sn-1 and sn-3 moiety groups of glyceryl tributyrate. Moreover, water dependence of lipase-catalysed reactions has been extensively reviewed by Adlercreutz [26] highlighting a critical role in increasing the local polarity when present in the region around the active site, stabilizing polar transition states, thus promoting reactions having such transition states. Water can also influence the stereoselectivity of the reactions by binding in substrate-binding pockets, thus interfering with the binding of one of the enantiomers of the substrate [47, 48].

The three contributions sum up into an asymmetric electrostatic potential (Figure 1f), on which the triglyceride is directly positioned with the oxygen of the ester moiety in position sn-1 on the vertical of Ser105 OH group (Figure 1e) at a distance of 10 Å. In our crystal structure, the diethyl-phosphonate inhibitor is bound to Ser105 similarly to the phosphonate inhibitor already obtained by Uppenberg et al., [18] (PDB code: 1LBS) with the phosphonate oxygen clearly pointing towards the oxyanion hole. Superimposing the two structures reveals that the triglyceride is correctly oriented with butyric acyl moiety towards the alcohol side of the cavity and with the glycerol backbone oriented towards the acyl side of the cavity, according to Uppenberg et al. [18] definitions. The ester moiety in position sn-1 has then a preferential position towards Ser105 OH group compared to acyl moiety in position sn-2 or sn-3, thus the upper level of the binding pocket,

by prepositioning the substrate can drive it towards an optimal orientation around the catalytic triad, throughout hydrophobic, hydrophilic interactions and a H-bond network.

In summary, in the tributyrin-CALB complex presented here, an extended network of waters tethers the glycerol backbone of TG's by forming H-bonds with the ester group oxygens. The result is a pre-alignment of the substrate towards the catalytic triad confirming the mediating role of water between substrate and enzyme.

Overall, this work clearly defines a limbus region of the active site of CALB, where substrate is recognized and sequestered in an intermediate state during the transition from the media into the depths of catalytic site. Given that the glycerol backbone is common to all triglycerides it can be inferred that in general, during hydrolysis, triglycerides will be aligned with the glycerol backbone in the same region of enzyme surface with adaptation given by different fatty acid length. This region works as a transition region, in which the first substrate-enzyme weak interactions, hydrophilic and hydrophobic, are established between the functional groups of amino acids and of the substrate, mediated by water molecules, favouring the transfer from the media down to the catalytic site for further processing.

**Accession Numbers:** The refined coordinate and structure factor files for the crystallographic structure have been deposited in the Protein Data Bank with assigned accession codes 6TP8 and NTK for glyceryl tributyrate (2,3-di(butanoyloxy)propyl butanoate).

**Acknowledgments.** LS is supported by the Università Politecnica delle Marche with the research grant PSA2017CIA (Ancona, Italy). MC is grateful to European Molecular Biology Laboratory (EMBL) for the beamtime.

## References


[1] H. Wong, The lipase gene family, Journal of Lipid Research 43(7) (2002) 993-999.
[2] M. Lotti, L. Alberghina, Lipases: molecular structure and function., in: J. Polaina, A.P. MacCabe (Eds.), Industrial Enzymes: Structure, Function and Applications, Springer, Dordrecht, The Netherlands, 2007, pp. 263-281.
[3] F. Hasan, A.A. Shah, A. Hameed, Industrial applications of microbial lipases, Enzyme and Microbial Technology 39(2) (2006) 235-251.
[4] K.-E. Jaeger, T. Eggert, Lipases for biotechnology, Current Opinion in Biotechnology 13 (2002) 390-397.
[5] N.S. Rios, B.B. Pinheiro, M.P. Pinheiro, R.M. Bezerra, J.C.S. dos Santos, L.R. Barros Gonçalves, Biotechnological potential of lipases from Pseudomonas: Sources, properties and applications, Process Biochemistry 75 (2018) 99-120.
[6] L. Sarda, P. Desnuelle, Actions of pancreatic lipase on esters in emulsions, Biochimica et Biophysica Acta 30 (1958) 513-521.
[7] R. Verger, 'interfacial activation' of lipases: facts and artifacts, TIBTECH 15 (1997) 32-38.
[8] R.D. Schmid, R. Verger, Lipases: Interfacial Enzymes with Attractive Applications, Angew. Chem. Int. Ed. 37 (1998) 1608-1633.
[9] A.M. Brzozowski, U. Derewendat, Z.S. Derewenda, G.G. Dodson, D.M. Lawson, J.P. Turkenburg, F. Bjorkling, B. Huge-Jensen, S.A. Patkar, L. Thim, A model for interfacial activation in lipases from the structure of a fungal lipase-inhibitor complex, Nature 351 (1991) 491-494.
[10] N.S. Rios, D.M.A. Neto, J.C.S. Dos Santos, P.B.A. Fechine, R. Fernandez-Lafuente, L.R.B. Goncalves, Comparison of the immobilization of lipase from Pseudomonas fluorescens on divinylsulfone or p-benzoquinone activated support, Int J Biol Macromol 134 (2019) 936-945.
[11] U.M.F. de Oliveira, L.J.B. Lima de Matos, M.C.M. de Souza, B.B. Pinheiro, J.C.S. Dos Santos, L.R.B. Goncalves, Efficient biotechnological synthesis of flavor esters using a low-cost biocatalyst with immobilized Rhizomucor miehei lipase, Mol Biol Rep 46(1) (2019) 597-608.
[12] E.A. Manoel, M.F.P. Ribeiro, J.C.S. dos Santos, M.A.Z. Coelho, A.B.C. Simas, R. Fernandez-Lafuente, D.M.G. Freire, Accurel MP 1000 as a support for the immobilization of lipase from Burkholderia cepacia : Application to the kinetic resolution of myo -inositol derivatives, Process Biochemistry 50(10) (2015) 1557-1564.
[13] E.A. Manoel, J.C. Dos Santos, D.M. Freire, N. Rueda, R. Fernandez-Lafuente, Immobilization of lipases on hydrophobic supports involves the open form of the enzyme, Enzyme Microb Technol 71 (2015) 53-7.
[14] J.C.S. Dos Santos, H.L. Bonazza, L. de Matos, E.A. Carneiro, O. Barbosa, R. Fernandez-Lafuente, L.R.B. Goncalves, H.B. de Sant' Ana, R.S. Santiago-Aguiar, Immobilization of CALB on activated chitosan: Application to enzymatic synthesis in supercritical and near-critical carbon dioxide, Biotechnol Rep (Amst) 14 (2017) 16-26.
[15] E.M. Anderson, K.M. Larsson, O. Kirk, One Biocatalyst – Many Applications: The Use of Candida Antarctica B-Lipase in Organic Synthesis, Biocatal. Biotransform. 16 (1998) 181-204.

[16] D. Rotticci, J.C. Rotticci-Mulder, S. Denman, T.r. Norin, K. Hult, Improved Enantioselectivity of a Lipase by Rational Protein Engineering, ChemBioChem 2 (2001) 766-770.
[17] J. Uppenberg, M.T. Hansen, S. Patkar, T.A. Jones, The sequence, crystal structure determination and refinement of two crystal forms of lipase B from Candida antarctica., Structure 2 (1994) 293-308.
[18] J. Uppenberg, N. Ohmer, M. Norin, K. Hult, G.J. Kleywegt, S. Patkar, V. Waagen, T. Anthomen, T.A. Jones, Crystallographic and Molecular-Modeling Studies of Lipase B from Candida antarctica Reveal a Stereospecificity Pocket for Secondary Alcohols, Biochemistry 34 (1995) 16838-16851.
[19] L. Brady, A.M. Brzozowski, Z.S. Derewenda, E. Dodson, G. Dodson, S. Tolley, J.P. Turkenburg, L. Christiansen, B. Huge-Jensen, L. Norskov, L. Thim, U. Menge, A serine protease triad forms the catalytic centre of a triacylglycerol lipase, Nature 343 (1990) 767-770.
[20] B. Stauch, S.J. Fisher, M. Cianci, Open and closed states of Candida antarctica lipase B: protonation and the mechanism of interfacial activation, J Lipid Res 56(12) (2015) 2348-58.
[21] M.R. Ganjalikhany, B. Ranjbar, A.H. Taghavi, T.T. Moghadam, Functional Motions of Candida antarctica Lipase B: A Survey through Open-Close Conformations, PloS One 7(7) (2012) e40327.
[22] P. Trodler, J. Pleiss, Modeling structure and flexibility of Candida antarctica lipase B in organic solvents, BMC structural biology 8 (2008) 9.
[23] M. Skjot, L. De Maria, R. Chatterjee, A. Svendsen, S.A. Patkar, P.R. Ostergaard, J. Brask, Understanding the plasticity of the alpha/beta hydrolase fold: lid swapping on the Candida antarctica lipase B results in chimeras with interesting biocatalytic properties, ChemBioChem 10(3) (2009) 520-7.
[24] T. Zisis, P.L. Freddolino, P. Turunen, M.C. van Teeseling, A.E. Rowan, K.G. Blank, Interfacial Activation of Candida antarctica Lipase B: Combined Evidence from Experiment and Simulation, Biochemistry 54(38) (2015) 5969-79.
[25] S.P. Benson, J. Pleiss, Self-Assembly Nanostructures of Triglyceride-Water Interfaces Determine Functional Conformations of Candida antarctica Lipase B, Langmuir 33(12) (2017) 3151-3159.
[26] P. Adlercreutz, Immobilisation and application of lipases in organic media, Chem Soc Rev 42(15) (2013) 6406-36.
[27] A. Salis, I. Svensson, M. Monduzzi, V. Solinas, P. Adlercreutz, The atypical lipase B from Candida antarctica is better adapted for organic media than the typical lipase from Thermomyces lanuginosa, Biochimica et Biophysica Acta (BBA) - Proteins and Proteomics 1646(1-2) (2003) 145-151.
[28] C. Touvrey, C. Courageux, V. Guillon, R. Terreux, F. Nachon, X. Brazzolotto, X-ray structures of human bile-salt activated lipase conjugated to nerve agents surrogates, Toxicology 411 (2019) 15-23.
[29] M. Cianci, G. Bourenkov, G. Pompidor, I. Karpics, J. Kallio, I. Bento, M. Roessle, F. Cipriani, S. Fiedler, T.R. Schneider, P13, the EMBL macromolecular crystallography beamline at the low-emittance PETRA III ring for high- and low-energy phasing with variable beam focusing, J Synchrotron Radiat 24(Pt 1) (2017) 323-332.

[30] W. Kabsch, XDS, Acta Crystallographica Section D: Biological Crystallography 66 (2010) 125-132.
[31] P. Evans, Scaling and assessment of data quality, Acta Crystallographica Section D: Biological Crystallography 62 (2006) 72-82.
[32] A.Vagin, A.Teplyakov, MOLREP: an automated program for molecular replacement, Journal of Applied Crystallography 30 (1997) 1022-1025.
[33] G.N. Murshudov, A.A. Vagin, E.J. Dodson, Refinement of Macromolecular Structures by the Maximum-Likelihood Method, Acta Crystallographica Section D: Biological Crystallography 53 (1996) 240-255.
[34] P. Emsley, B. Lohkamp, W.G. Scott, K. Cowtan, Features and development of Coot, Acta Crystallographica Section D: Biological Crystallography 66(4) (2010) 486-501.
[35] R.P. Joosten, F. Long, G.N. Murshudov, A. Perrakis, The PDB_REDO server for macromolecular structure model optimization, IUCrJ 1(Pt 4) (2014) 213-20.
[36] P.D. Adams, P.V. Afonine, G. Bunkóczi, V.B. Chen, I.W. Davis, N. Echols, J.J. Headd, L.-W. Hung, G.J. Kapral, R.W. Grosse-Kunstleve, A.J. McCoy, N.W. Moriarty, R. Oeffner, R.J. Read, D.C. Richardson, J.S. Richardson, T.C. Terwilliger, P.H. Zwart, PHENIX: a comprehensive Python-based system for macromolecular structure solution., Acta Crystallographica Section D: Biological Crystallography 66 (2010) 213-221.
[37] E. Krissinel, K. Henrick, Inference of Macromolecular Assemblies from Crystalline State, Journal of Molecular Biology 373 (2007) 774-797.
[38] D.L. Nelson, M. Cox, A.L. Lehninger, Lehninger Principles of Biochemistry: International Edition, 7th ed., W.H. Freeman and Company ; Houndmills, Basingstoke : Macmillan Higher Education, New York, NY, 2017.
[39] J. Uppenberg, S. Patkar, T. Bergfors, T.A. Jones, Crystallization and preliminary X-ray studies of lipase B from Candida antarctica, J. Mol. Biol. 235 (1994) 790-792.
[40] Z. Qian, J.R. Horton, X. Cheng, S. Lutz, Structural redesign of lipase B from Candida antarctica by circular permutation and incremental truncation, J Mol Biol 393(1) (2009) 191-201.
[41] B. Luan, R. Zhou, A novel self-activation mechanism of Candida antarctica lipase B, Physical Chemistry Chemical Physics 19 (2017) 15709-15714.
[42] G.H. Peters, O.H. Olsen, A. Svendsen, R.C. Wade, Theoretical Investigation of the Dynamics of the Active Site Lid in Rhizomucor miehei Lipase, Biophysical Journal 71 (1996) 119-129.
[43] A. Sanchez, J. Cru, N. Rueda, J.C.S.d. Santob, R. Torres, C. Ortiz, R. Villalonga, R. Fernandez-Lafuente, Inactivation of immobilized trypsin under dissimilar conditions produces trypsin molecules with different structures, Rsc Advances 6 (2016) 27329-27334.
[44] J.M. Palomo, G. Muñoz, G. Fernández-Lorente, C. Mateo, R. Fernández-Lafuente, J.M. Guisán, Interfacial adsorption of lipases on very hydrophobic support (octadecyl–Sepabeads): immobilization, hyperactivation and stabilization of the open form of lipases, Journal of Molecular Catalysis B: Enzymatic 19-20 (2002) 279–286.
[45] F.A. Lage, J.J. Bassi, M.C. Corradini, L.M. Todero, J.H. Luiz, A.A. Mendes, Preparation of a biocatalyst via physical adsorption of lipase from Thermomyces lanuginosus on hydrophobic support to catalyze biolubricant synthesis by esterification reaction in a solvent-free system, Enzyme Microb Technol 84 (2016) 56-67.

[46] E. Rogalska, C. Cudrey, F. Ferrato, R. Verger, Stereoselective Hydrolysis of Triglycerides by Animal and Microbial Lipases, Chirality 5 (1993) 24-30.
[47] V. Léonard-Nevers, Z. Marton, S. Lamare, K. Hult, M. Graber, Understanding water effect on Candida antarctica lipase B activity and enantioselectivity towards secondary alcohols, Journal of Molecular Catalysis B: Enzymatic 59(1-3) (2009) 90-95.
[48] V. Leonard, L. Fransson, S. Lamare, K. Hult, M. Graber, A water molecule in the stereospecificity pocket of Candida antarctica lipase B enhances enantioselectivity towards pentan-2-ol, Chembiochem 8(6) (2007) 662-7.

Data collection and processing. Highest resolution bin are reported in parenthesis.

**Table 1**

| | |
|---|---|
| Wavelength (Å) | 0.824 |
| Resolution range (Å) | 67.69 - 1.55 (1.605 - 1.55) |
| Space group | $C222_1$ |
| Unit cell (a, b, c, (Å); α, β, γ, (°)) | 89.42, 156.65, 138.08, 90 90 90 |
| Total reflections | 1049281 (48047) |
| Unique reflections | 138806 (13617) |
| Multiplicity | 7.6 (7.2) |
| Completeness (%) | 99.18 (98.05) |
| Wilson B-factor ($Å^2$) | 18.90 |
| $R_{merge}$ | 0.121 (1.46) |
| $R_{meas}$ | 0.140 (1.70) |
| $R_{pim}$ | 0.050 (0.877) |
| Mean (I) half-set correlation CC(1/2) | 0.997 (0.550) |
| Mean I/σ(I) | 8.4 (1.0) |
| Reflections used in refinement | 138776 (13610) |
| Reflections used for R-free | 7001 (694) |

**Table 2**. Refinement statistics. $R_{free}$ is calculated using 5% of the total reflections that were randomly selected and excluded from refinement.

| | |
|---|---|
| Number of monomers in the asymmetric unit | 3 |
| $R_{work}$ (%) | 16.3 (29.7) |
| $R_{free}$ (%) | 19.2 (31.3) |
| Number of non-hydrogen atoms | 8652 |
| macromolecules | 7041 |
| ligands | 150 |
| solvent | 1461 |
| Protein residues | 951 |
| RMS(bonds) (Å) | 0.007 |
| RMS(angles) (°) | 1.28 |
| Ramachandran favored (%) | 97.57 |
| Ramachandran allowed (%) | 2.22 |
| Ramachandran outliers (%) | 0.21 |
| Rotamer outliers (%) | 0.26 |
| Average B-factor ($Å^2$) | 21.85 |

**Figure 1**. Structural details of *Candida Antarctica* Lipase B: a) Ribbon diagram of the homodimer with one molecule of glycerol tributyrate bound (depicted in black) shared between the two monomers; b, c) the OMIT map (blue mesh; contour level 3.0σ, calculated without the residues) at 1.55 Å resolution for the glycerol tributyrate bound between monomer A and B, and C and C' respectively, calculated with Fourier coefficients $F_o$-$F_c$ and phases from the refinement of CALB structure prior to the addition of any ligand molecules; d) the active sites of monomer A (left, black residue labels) and monomer B (right, blue residue labels) inhibited by the bound diethyl-phosphonate (DEP) and sharing the bound glycerol tributyrate molecule (T3B) at the top of the cleft with highlighted the residues (fat bonds, oxygen atom in red and nitrogen atom in dark blue), within 4 Å from T3B and DEP; e) relative side position of glycerol tributyrate to the active site, α-helix 5, α-helix 10, and water network; f) electrostatic potential of CALB surface. Red areas have a negative potential, blue areas a positive potential, white areas are neutral.

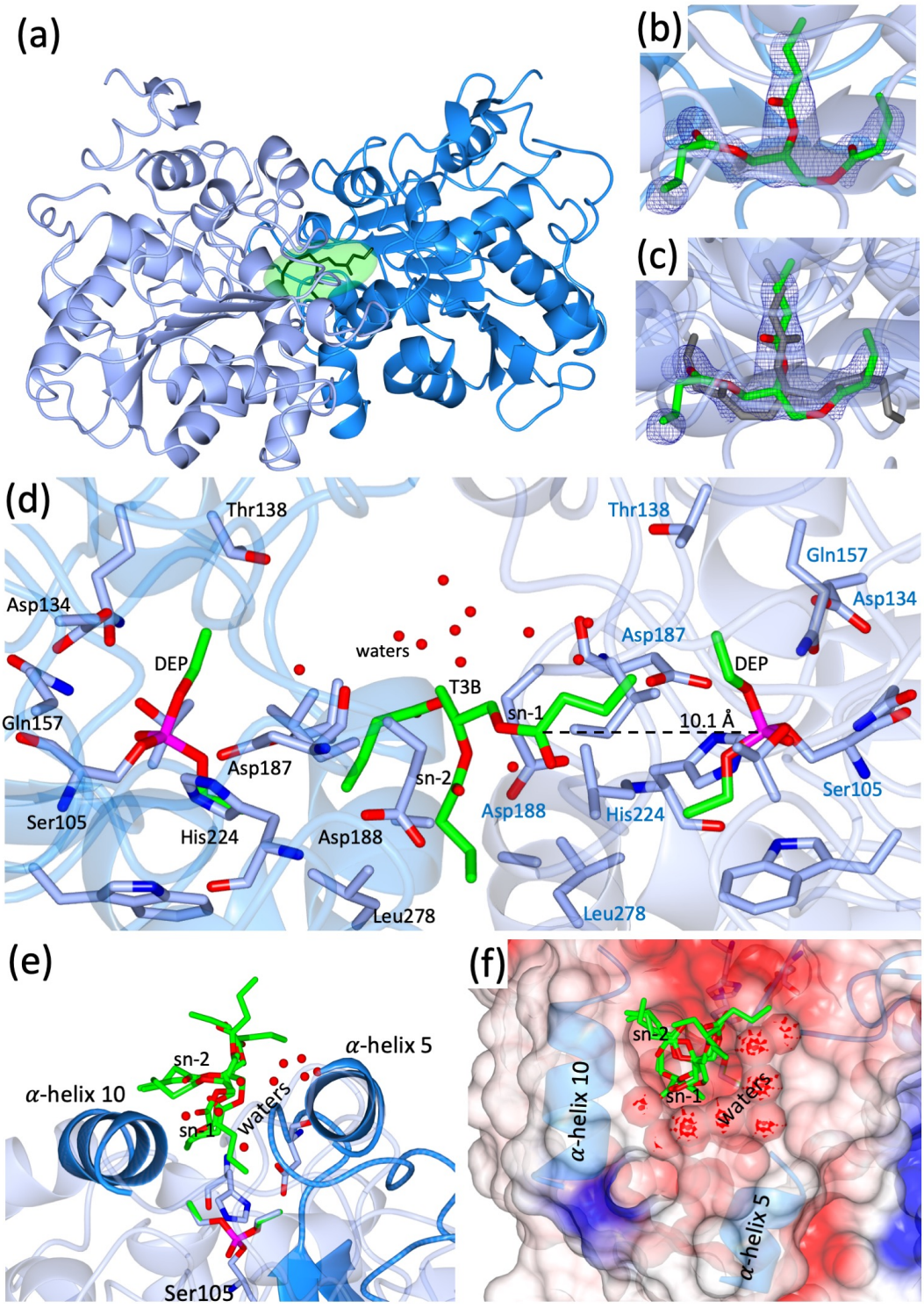


**Figure 1**. Silvestrini & Cianci, 2020